

Pressure induced topological quantum phase transition in Weyl semimetal T_d -MoTe₂

Z. Guguchia,^{1,*} A.M. dos Santos,² F.O. von Rohr,^{3,4} J.J. Molaison,² S. Banerjee,⁵ D. Rhodes,⁶ J.-X. Yin,⁷ R. Khasanov,¹ J. Hone,⁸ Y.J. Uemura,⁹ M.-Z. Hasan,⁷ H. Luetkens,¹ E.S. Bozin,¹⁰ and A. Amato¹

¹Laboratory for Muon Spin Spectroscopy, Paul Scherrer Institute, CH-5232 Villigen PSI, Switzerland

²Neutron Scattering Division, Oak Ridge National Laboratory, Oak Ridge, Tennessee 37831, USA

³Department of Chemistry, University of Zurich, CH-8057 Zurich, Switzerland

⁴Department of Physics, University of Zurich, CH-8057 Zurich, Switzerland

⁵Condensed Matter Physics and Materials Science Department,
Brookhaven National Laboratory, Upton, NY 11973, USA

⁶Department of Materials Science and Engineering,
University of Wisconsin-Madison, 1509 University Ave, Madison, WI 53706, USA

⁷Laboratory for Topological Quantum Matter and Spectroscopy,

Department of Physics, Princeton University, Princeton, New Jersey 08544, USA

⁸Department of Mechanical Engineering, Columbia University, New York, NY 10027, USA

⁹Department of Physics, Columbia University, New York, NY 10027, USA

¹⁰Condensed Matter Physics and Materials Science Division,
Brookhaven National Laboratory, Upton, NY 11973, USA

We report the pressure ($p_{max} \simeq 1.5$ GPa) evolution of the crystal structure of the Weyl semimetal T_d -MoTe₂ by means of neutron diffraction experiments. We find that the fundamental non-centrosymmetric structure T_d is fully suppressed and transforms into a centrosymmetric $1T'$ structure at a critical pressure of $p_{cr} \sim 1.2$ GPa. This is strong evidence for a pressure induced quantum phase transition (QPT) between topological to a trivial electronic state. Although the topological QPT has strong effect on magnetoresistance, it is interesting that the superconducting critical temperature T_c , the superfluid density, and the SC gap all change smoothly and continuously across p_{cr} and no sudden effects are seen concomitantly with the suppression of the T_d structure. This implies that the T_c , and thus the SC pairing strength, is unaffected by the topological QPT. However, the QPT requires the change in the SC gap symmetry from non-trivial s^{+-} to a trivial s^{++} state, which we discuss in this work. Our systematic characterizations of the structure and superconducting properties associated with the topological QPT provide deep insight into the pressure induced phase diagram in this topological quantum material.

I. INTRODUCTION

Transition metal dichalcogenides (TMDs) have attracted a lot of attention due to their fascinating physics and promising functional applications [1–18]. TMDs share the same formula, MX_2 , where M is a transition metal (for example, Mo or W) and X is a chalcogenide atom (S, Se and Te). These compounds typically crystallize in a group of related structure types, including $1T'$ - and T_d -type lattices [19–22] as shown in Figure 1. The $1T'$ phase is monoclinic lattice and comprises a distorted octahedral coordination of the metal ions, exhibiting pseudo-hexagonal layers with zig-zag edge sharing metal chains. The T_d phase is orthorhombic and both $1T'$ and T_d structures are related by a slight change in the stacking pattern of the layers. Both $1T'$ - and T_d are semimetals. The central difference between these two structures is that the $1T'$ structure exhibits the inversion symmetric space group $P2_1/m$, while the T_d phase belongs to the non-centrosymmetric space group $Pmn2_1$.

MoTe₂ exhibits a $1T'$ - T_d structural phase transition, on warming, at $T_{str} \sim 280$ K [17]. MoTe₂, with the non-

inversion symmetric orthorhombic T_d phase, is a type-II Weyl semimetal [1, 2, 4–10], where the Weyl Fermions emerge at the boundary between electron and hole pockets. High field quantum oscillation study of the magnetoresistance (MR) for T_d -MoTe₂, revealed a nontrivial π Berry's phase, which is a distinguished feature of surface states [23]. Non-saturating magnetoresistance [11–14], and superconductivity [15–17] were also observed in T_d -MoTe₂. Hence, T_d -MoTe₂ represents a rare example of a material with both a topologically non-trivial band structure and superconductivity [24]. The superconducting critical temperature of T_d -MoTe₂ is $T_c \simeq 0.1$ K [17] at ambient conditions. The application of hydrostatic pressure [17, 25], the substitution of Te ion by S [26] or the creation of Te-vacancies can dramatically enhance T_c and lead to a dome-shaped superconductivity in T_d -MoTe₂. Experimental signatures of topological superconducting order parameter s^{+-} within T_d structure were reported by recent muon-spin rotation μ SR experiments and T_d -MoTe₂ is claimed to be a candidate material for a time reversal invariant topological (Weyl) superconductor (TSC) [25, 27–29]. These are special families of materials with unique electronic states, a full pairing gap in the bulk and gapless surface states consisting of Majorana fermions (MFs) [27–29]. Therefore, the combination of Weyl physics and superconductivity may support Majorana or other exotic surface states in view of

*Electronic address: zurab.guguchia@psi.ch

their topological nature. These states are of fundamental interest and may eventually be utilised for Quantum computing. For this reason, there is an ongoing effort aimed at achieving superconductivity in such materials and investigating their properties, either with the use of the proximity effect or by other means.

Besides the enhancement of T_c , pressure causes the suppression of the non-centrosymmetric orthorhombic T_d structure, as it was reported by resistivity experiments [17]. However, resistivity is rather indirect probe for the structural transition and relies only on a weak anomaly, appearing around the structural phase transition T_{str} . In order to understand the role of the crystal structure for the occurrence of superconductivity in MoTe_2 , it is essential to directly investigate the structure as a function of pressure using a conventional structural probe such as neutron diffraction. Since pressure has strong effect on superconductivity in MoTe_2 , by investigating structural properties under pressure we aim to find the correlation between pressure induced structural and electronic quantum phase transitions in this important TMD system MoTe_2 .

II. EXPERIMENTAL DETAILS

High quality single crystals and polycrystalline samples were obtained by mixing of molybdenum foil (99.95 %) and tellurium lumps (99.999+%) in a ratio of 1:20 in a quartz tube and sealed under vacuum. The reagents were heated to 1000°C within 10 h. They dwelled at this temperature for 24 h, before they were cooled to 900°C within 30 h (polycrystalline sample) or 100 h (single crystals). At 900°C the tellurium flux was spinned-off and the samples were quenched in air. The obtained MoTe_2 samples were annealed at 400°C for 12 h to remove any residual tellurium.

High pressure neutron diffraction experiments on T_d - MoTe_2 were carried out at SNAP beamline of Spallation Neutron Source at Oak Ridge National Laboratory. SNS operates at 60 Hz, and SNAP instrument utilizes time of flight diffraction mode. The center wavelength was set to 2.1 Å, corresponding to an incident wavelength spectrum from 0.5 Å to 3.5 Å. Two banks of detectors cover ± 22.5 deg in angular range in and out of plane. Their center was placed at 50 deg scattering angle. This configuration limits the accessible Q-range, but provides increased counting statistics in the region of interest that is most relevant for discriminating between T_d and $1T'$ phases. Pressures up to 1.6 GPa were generated in a single wall piston-cylinder type of cell made of CuBe material, especially designed to perform neutron diffraction experiments under pressure. Daphne oil was used as a pressure transmitting medium. The pressure was always applied at room temperature, followed by cooling the sample to the base temperature (15 K) and carrying out temperature dependent measurements on warming. The pressure was measured by tracking the Raman spectrum of lead

powder as a function of pressure. The diffraction experiments were done on the samples from the same batch as the ones, which we previously studied by μSR experiments [25].

Total scattering measurements were carried out on the XPD (28-ID-2) beamline at the National Synchrotron Light Source II (NSLS-II), Brookhaven National Laboratory. A finely ground powder of MoTe_2 was prepared in an inert Argon chamber, and sealed in 1.02mm (OD) polyimide capillary. Diffraction patterns were collected in a Debye-Scherrer geometry with an X-ray energy of 67.13 keV ($\lambda = 0.1847$ Å) using a large-area 2D PerkinElmer detector (2048² pixels with 200 μm^2 pixel size). The detector was mounted with a sample-to-detector distance of 345 mm, to achieve a balance between q -resolution and q -range. The sample was measured at 100K and 300K using an Oxford CS-700 cryostream for temperature control, allowing ample time for the material to thermalize. The experimental geometry, 2θ range, and detector orientation were calibrated by measuring a polycrystalline nickel standard directly prior to data collection, with the experimental geometry parameters refined using the PyFAI program [30].

III. RESULTS

The orthorhombic (T_d) to monoclinic ($1T'$) structural phase transition in the MoTe_2 sample at ambient pressure was confirmed by the X-ray total scattering measurements, shown in Fig. 2. In Figure 2a-b, we index the Bragg profile and compare the raw diffraction patterns measured at 100 K and 300 K to powder diffraction patterns calculated from the candidate models using the program VESTA [31]. We plot the data over a d -range where the $1T'$ and T_d models have Bragg peaks that are well resolved from one another to highlight distinguishable features that differ between the phases in the measured XRD pattern. The strongest structural signatures of the transition are seen as splitting of the orthorhombic (113) and (112) reflections in monoclinic phase, as it was also reported for WTe_2 [32, 33].

Confirming the low temperature T_d structure as well as the signature of the structural phase transition in MoTe_2 , we proceed with observations made by neutron scattering measurements under hydrostatic pressure. The most intense peak is (112) at d -spacing of 2.8 Å, which was monitored at various temperatures and pressures. The results are shown in Figure 3a-d. Figure 3a shows the temperature evolution of the (112) peak at ambient pressure. The peak splits above 285 K, consistent with the T_d to $1T'$ structural phase transition and experimental observations of XRD experiment. The transition temperature $T_{str} \sim 290$ K is higher than the one $T_{str} \sim 250$ K, originally reported from transport experiments [17]. Upon increasing pressure, the temperature, above which the peak splits, decreases, pointing to the suppression of T_{str} with pressure. At 1.6 GPa, no single orthorhombic (112)

peak is observed within the resolution of our measurement, and monoclinic peaks are observed at all temperature, indicating the full suppression of the orthorhombic T_d structure at this pressure. Figure 4 shows the pressure dependence of the structural phase transition temperature T_{str} , superimposed with the dependence of SC critical temperature (taken from Reference [25]), measured on the sample from the same batch. This phase diagram shows that the orthorhombic to monoclinic quantum phase transition ($T=0$) takes place at the critical pressure of $p_{\text{cr}} \sim 1.2$ GPa, but T_c continues to increase smoothly and persists well beyond the p_{cr} . The suppression of the orthorhombic phase as well as the value of the critical pressure is in a very good agreement with very recent single crystal neutron diffraction [34].

A. Discussion

What is the significance of such a strong negative pressure effect on T_d structure and the structural QPT in Weyl semimetal MoTe₂? Let us start with the fact that T_d structure breaks inversion symmetry, while $1T'$ is inversion symmetric. As low pressure as 1.2 GPa is sufficient to wipe out non-inversion symmetric T_d phase. One common point of view in MoTe₂, mostly supported by calculations, is that Weyl Fermions and their underlying non-trivial band topology, exist only in T_d phase. Hence, the structural QPT between T_d and $1T'$ corresponds to the quantum phase transition between topologically non-trivial and a trivial band structure. One of the consequences of such a topological quantum phase transition is the strong suppression of the magnetoresistance with increasing pressure. For the pressure values $p > p_{\text{cr}}$, MR is fully suppressed [35]. This was explained by the fact that MR is very sensitive to a hole-to-electron concentration ratio N_h/N_e and by driving the system into $1T'$ phase, the strong deviation from the optimal ratio takes place, leading to the suppression of MR. In fact, MR is strongly suppressed already well below p_{cr} , which is ascribed to the presence of a significant band tilting around the Weyl nodes under pressure within the T_d phase, as shown by calculations [34]. When the Weyl nodes fully disappear at p_{cr} , than this leads to the full suppression of MR [35].

Although the topological QPT has a strong effect on MR [35], it is interesting that the superconducting critical temperature T_c as well as the SC gap Δ (Figure 4, only the large SC gap [25] is shown) changes smoothly across p_{cr} and no sudden effects are seen due to the suppression of T_d structure. This implies that the T_c and thus the SC pairing strength is unaffected by the topological QPT. This can be understood in light of Hall conductivity measurements, showing that a pair of electron and hole bands are dominant in the T_d structure and the carrier densities on these bands increase smoothly with pressure and no sudden changes are observed across p_{cr} . Having this in mind as well as our previous work [25],

according to which T_c scales with the superconducting carrier density, one can understand the insensitivity of T_c to topological QPT.

Since there is only a subtle change in the Fermi surface (FS) topology [35] at p_{cr} , bulk SC quantities such as T_c , Δ and the superfluid density, are not affected by QPT. However, one more physical parameter that we should consider is the symmetry of the SC order parameter. Previously, we showed that the superconductor T_d -MoTe₂ represents a time-reversal-invariant Weyl semimetal, which has broken inversion symmetry below p_{cr} . Moreover, it is a two-gap superconductor both below and above p_{cr} (we have one point just above p_{cr}) and the gaps are momentum independent on each Fermi surface. Following the theoretical studies of time-reversal-invariant topological superconductivity in Weyl semimetals, the nontrivial Berry curvature at the FSs of WSMs allows the TSC to be realized for a pairing function with no special momentum dependence. A simple formula [27–29] relates the FS Chern number to the topological invariant ν for a time-invariant TSC, considering a set of FSs with Chern numbers C_j :

$$\nu = \frac{1}{2} \sum_{j \in \text{FS}} C_j \text{sgn}(\Delta_j), \quad (1)$$

where Δ_j is the pairing gap function on the j -th FS. A TSC is implied by $\nu \neq 0$. Therefore, as previously discussed [27], a necessary condition for TSC is that Δ_1 and Δ_2 have opposite signs. Thus, T_d -MoTe₂ is a natural candidate for topological s^{+-} SC order parameter within non-centrosymmetric T_d structure since the non-trivial Chern number is already provided by the band structure. The s^{+-} order parameter in T_d -MoTe₂ is also supported by strong disorder dependence of T_c [13, 25]. It was shown that the violation of inversion symmetry stabilises the state where the ferromagnetic exchange coupling is greater than or comparable to the repulsive density-density interactions, which than results in topological superconducting state [27]. Once the inversion symmetry is recovered than the TSC is quenched. This means that at pressure above p_{cr} , where crystal structure has inversion symmetry, the trivial s^{++} state (where Δ_1 and Δ_2 have the same sign) should be favoured over the topological s^{+-} state. While a direct proof for such a pressure induced QPT between s^{+-} and s^{++} states in MoTe₂ is clearly lacking, we conjecture this based on solid experimental evidence gleaned from the quantum phase transition between non-centrosymmetric to a centrosymmetric structure and our previous observation of two-gap superconductivity. This paves the way for rigorous experimental as well as theoretical explorations of this idea. One immediately useful study would be that of the effects of impurities on superconductivity above p_{cr} . This should discriminate/differentiate between topological s^{+-} and ordinary s^{++} state, since according to the theoretical proposal TSC is much more sensitive to disorder than the ordinary s^{++} superconductivity.

IV. CONCLUSIONS

In conclusion, we studied the hydrostatic pressure evolution of a monoclinic $1T'$ to orthorhombic T_d structural phase transition temperature T_{str} using neutron diffraction. The quantum phase transition from non-centrosymmetric T_d to a centrosymmetric $1T'$ structure is observed under pressure with the critical pressure of $p_{\text{cr}} \sim 1.2$ GPa. No obvious impact of such a QPT on SC critical temperature, the SC gap(s) and the superfluid density is observed, suggesting that only subtle changes take place in the Fermi surface across p_{cr} despite the transition from a topological to a topological-trivial band structure. However, due to the recovery of inversion symmetry above p_{cr} , the trivial s^{++} superconducting state should be favoured over the topological s^{+-} state. Hence, this system may likely be the first known example of a pressure induced change between topological ($p < p_{\text{cr}}$) and trivial ($p > p_{\text{cr}}$) SC states.

V. ACKNOWLEDGMENTS

A portion of this research used resources at the Spallation Neutron Source, a DOE Office of Science User Facility operated by the Oak Ridge National Laboratory.

Work at Brookhaven National Laboratory was supported by US DOE, Office of Science, Office of Basic Energy Sciences under contract DE-SC0012704. Research at Columbia was supported by US NSF DMR-1610633 and the Reimei Project of the Japan Atomic Energy Agency. Z. Guguchia gratefully acknowledges the financial support by the Swiss National Science Foundation (SNF fellowship P300P2-177832). The work at the University of Zurich was supported by the Swiss National Science Foundation under Grant No. PZ00P2-174015.

VI. COMPETING INTERESTS

The authors declare that they have no competing interests.

VII. DATA AND MATERIALS AVAILABILITY

All data supporting the stated conclusions of the manuscript are in the paper. Additional data are available from the authors upon request.

-
- [1] Soluyanov, A. et al. Type II Weyl Semimetals. *Nature* **527**, 495 (2015).
 - [2] Sun, Y., Wu, S.C., Ali, M.N., Felser, C., and Yan, B. Prediction of Weyl semimetal in orthorhombic MoTe_2 . *Phys. Rev. B* **92**, 161107 (2015).
 - [3] Hao Zheng, Guang Bian, Guoqing Chang, Hong Lu, Su-Yang Xu, Guangqiang Wang, Tay-Rong Chang, Song-tian Zhang, Ilya Belopolski, Nasser Alidoust, Daniel S. Sanchez, Fengqi Song, Horng-Tay Jeng, Nan Yao, Arun Bansil, Shuang Jia, Hsin Lin, M. Zahid Hasan, Atomic-scale visualization of quasiparticle interference on a type-II Weyl semimetal surface. *Phys. Rev. Lett.* **117**, 266804 (2016).
 - [4] Wang, Z. et al. MoTe_2 : A Type-II Weyl Topological Metal. *Phys. Rev. Lett.* **117**, 056805 (2016).
 - [5] A.P. Weber et. al., Spin-Resolved Electronic Response to the Phase Transition in MoTe_2 . *Phys. Rev. Lett.* **121**, 156401 (2018).
 - [6] Kourtis, S., Li, J., Wang, Z., Yazdani, A. and Bernevig, B. A. Universal signatures of Fermi arcs in quasiparticle interference on the surface of Weyl semimetals. *Phys. Rev. B* **93**, 041109 (2016).
 - [7] Deng, K et al., Experimental observation of topological Fermi arcs in type-II Weyl semimetal MoTe_2 . *arXiv:1603.08508v2* (2016).
 - [8] Xu, N et. al., Discovery of Weyl semimetal state violating Lorentz invariance in MoTe_2 .
 - [9] L. Huang, T.M. McCormick, M. Ochi, Z. Zhao, M.-T. Suzuki, R. Arita, Y. Wu, D. Mou, H. Cao, J. Yan, N. Trivedi, and A. Kaminski. Spectroscopic evidence for a type II Weyl semimetallic state in MoTe_2 . *Nature Mater.* **15**, 1155 (2016).
 - [10] Tamai, A. and Wu, Q. S. and Cucchi, I. and Bruno, F. Y. and Riccò, S. and Kim, T. K. and Hoesch, M. and Barreteau, C. and Giannini, E. and Besnard, C. and Soluyanov, A. A. and Baumberger, F. Fermi Arcs and Their Topological Character in the Candidate Type-II Weyl Semimetal MoTe_2 . *Phys. Rev. X* **6**, 031021 (2016).
 - [11] Xu, X., Yao, W., Xiao, D. and Heinz, T. F. Spin and pseudospins in layered transition metal dichalcogenides. *Nat. Phys.* **10**, 343 (2014).
 - [12] Ali, M. N. et al. Large, non-saturating magnetoresistance in WTe_2 . *Nature* **514**, 205 (2014).
 - [13] Rhodes, D. et al. Impurity dependent superconductivity, Berry phase and bulk Fermi surface of the Weyl type-II semi-metal candidate MoTe_2 . *arXiv:1605.09065v3* (2016).
 - [14] Zhu, Z. et al. Quantum oscillations, thermoelectric coefficients, and the fermi surface of semimetallic WTe_2 . *Phys. Rev. Lett.* **114**, 176601 (2015).
 - [15] Pan, X.-C. et al. Pressure-driven dome-shaped superconductivity and electronic structural evolution in tungsten ditelluride. *Nat. Commun.* **6**, 7805 (2015).
 - [16] Kang, D. et al. Superconductivity emerging from suppressed large magnetoresistant state in WTe_2 . *Nat. Commun.* **6**, 7804 (2015).
 - [17] Y. Qi *et al.*, Superconductivity in Weyl semimetal candidate MoTe_2 . *Nat. Comm.* **7**, 11038 (2016).
 - [18] Absence of local fluctuating dimers in superconducting $\text{Ir}_{1-x}(\text{Pt,Rh})_x\text{Te}_2$. R. Yu, S. Banerjee, H.C. Lei,

- R. Sinclair, M. Abeykoon, H.D. Zhou, C. Petrovic, Z. Guguchia, and E. S. Bozin. Phys. Rev. B **97**, 174515 (2018).
- [19] Clarke, R., Marseglia, E. and Hughes, H. P. A low-temperature structural phase transition in b-MoTe₂. Philos. Mag. B **38**, 121-126 (1978).
- [20] Puotinen, D. and Newnham, R. E. The crystal structure of MoTe₂. Acta Crystallogr. **14**, 691-692 (1961).
- [21] Zandt, T., Dwelk, H., Janowitz, C. and Manzke, R. Quadratic temperature dependence up to 50 K of the resistivity of metallic MoTe₂. J. Alloys Compd. **442**, 216-218 (2007).
- [22] Brown, B. E. The crystal structures of WTe₂ and high-temperature MoTe₂. Acta Crystallogr. **20**, 268-274 (1966).
- [23] X. Luo, F.C. Chen, J.L. Zhang, Q.L. Pei, G.T. Lin, W.J. Lu, Y.Y. Han, C.Y. Xi, W.H. Song, and Y.P. Sun, T_d-MoTe₂: A possible topological superconductor. Applied Physics Letters **109**, 102601 (2016).
- [24] Lukas Muechler, Zurab Guguchia, Jean-Christophe Orain, Jürgen Nuss, Leslie M. Schoop, Ronny Thomale, Fabian O. von Rohr. Superconducting order parameter of the nodal-line semimetal NaAlSi. APL Materials **7**, 121103 (2019).
- [25] Z. Guguchia, F. von Rohr, Z. Shermadini, A. T. Lee, S. Banerjee, A. R. Wieteska, C. A. Marianetti, B. A. Frandsen, H. Luetkens, Z. Gong, S. C. Cheung, C. Baines, A. Shengelaya, G. Taniashvili, A. N. Pasupathy, E. Morenzoni, S. J. L. Billinge, A. Amato, R. J. Cava, R. Khasanov and Y. J. Uemura, Nat. Comm. **8**, 1082 (2017).
- [26] F.C. Chen, X. Luo, R.C. Xiao, W.J. Lu, B. Zhang, H.X. Yang, J.Q. Li, Q.L. Pei, D.F. Shao, R.R. Zhang, L.S. Ling, C.Y. Xi, W.H. Song and Y.P. Sun, Superconductivity enhancement in the S-doped Weyl semimetal candidate MoTe₂. Appl. Phys. Lett. **109**, 162601 (2016).
- [27] P. Hosur, X. Dai, Z. Fang, and X.-L. Qi, Time-reversal-invariant topological superconductivity in doped Weyl semimetals. Phys. Rev. B **90**, 045130 (2014).
- [28] Y. Ando and L. Fu, Topological Crystalline Insulators and Topological Superconductors: From Concepts to Materials Annual Review of Condensed Matter Physics **6**, 361 (2015).
- [29] A.G. Grushin, Phys. Rev. D **86**, 045001 (2012).
- [30] Kieffer, J. and Karkoulis, D. *PyFAI*, a versatile library for azimuthal regrouping. Journal of Physics: Conference Series **425**, 202012 (2013).
- [31] Momma, K. and Izumi, F., VESTA: a three-dimensional visualization system for electronic and structural analysis. Journal of Applied Crystallography **41**, 653 (2008).
- [32] Lu, Pengchao et. al., Origin of the superconductivity of WTe₂ under pressure. Phys. Rev. B **94**, 224512 (2016).
- [33] Y. Tao, J.A. Schneeloch, A.A. Aczel, and D. Louca, T_d to 1T structural phase transition in WTe₂ Weyl semimetal. arXiv:2003.09489v1 (2020).
- [34] S. Dissanayake, C. Duan, J. Yang, J. Liu, M. Matsuda, C. Yue, J.A. Schneeloch, J.C.Y. Teo and D. Louca, Electronic band tuning under pressure in MoTe₂ topological semimetal. NPJ Quantum Materials **4**, 45 (2019).
- [35] S. Lee, J. Jang, S.-H. Kim, S.-G. Jung, J. Kim, S. Cho, S.W. Kim, J.Y. Rhee, K.-S. Park, and T. Park, Origin of extremely large magnetoresistance in the candidate type-II Weyl semimetal MoTe_{2-x}. Scientific Reports **8**, 13937 (2018).

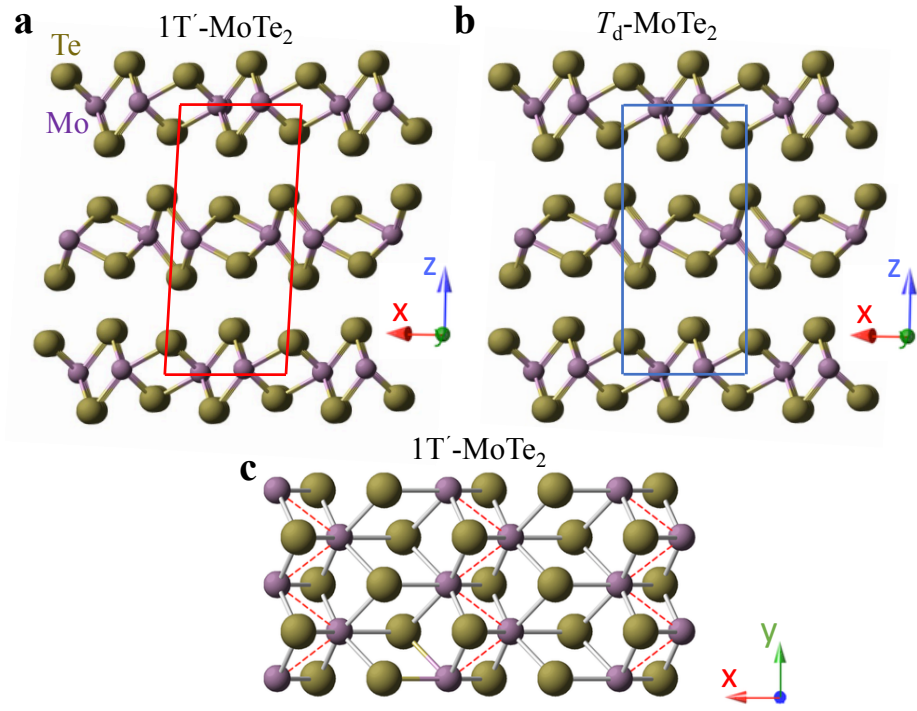


Figure 1: (Color online) Structural representations (side view) of the centrosymmetric 1T' (a) and non-centrosymmetric T_d (b) structures for MoTe₂. (c) Top view of monolayer constructed from distorted octahedral coordination.

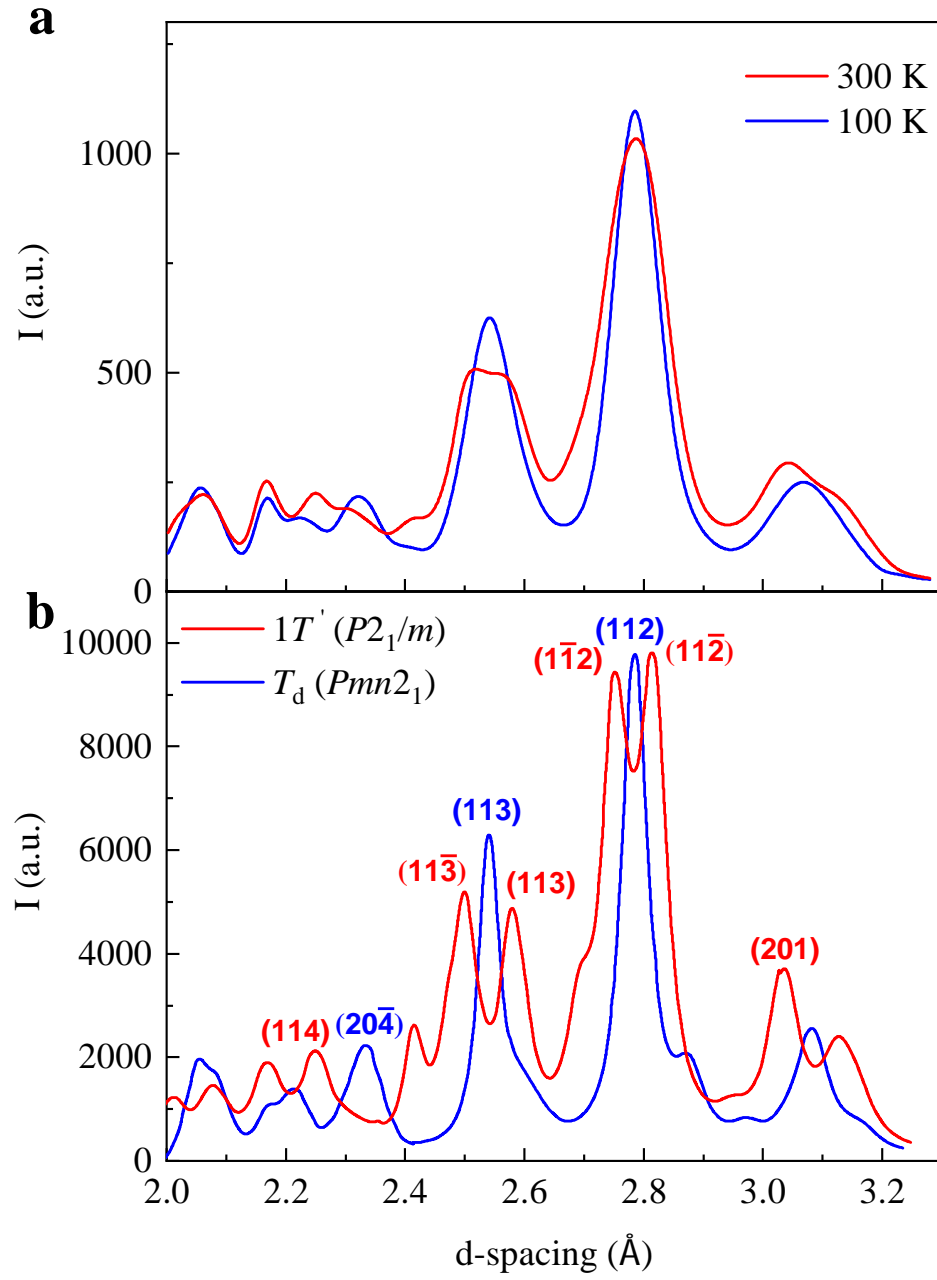


Figure 2: (Color online) (a) Raw diffraction patterns for 300K and 100K measurements using an incident wavelength of $\lambda = 0.18470$ \AA . (b) Bragg profile calculated from unmodified candidate structures. Solid curves in red and blue are the Bragg peaks calculated from the reflections (sharp lines), broadened uniformly with an FWHM=0.1 in 2θ ($=0.059\text{\AA}^{-1}$ in Q). The orthorhombic (113) reflection measured at 100K, splits into the $(11\bar{3})$ and (113) at 300K.

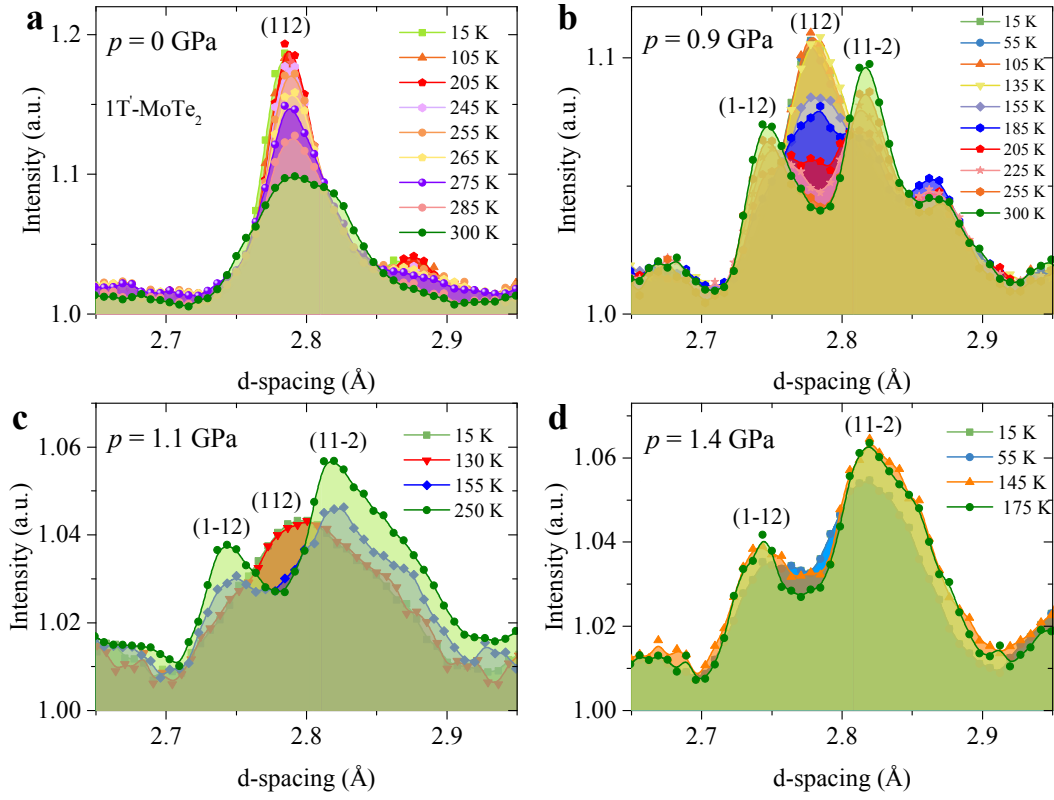


Figure 3: (Color online) The temperature dependence of (112) Bragg peak of MoTe_2 , recorded at various pressures: (a) $p = 0$ GPa, (b) $p = 0.9$ GPa, (c) $p = 1.1$ GPa, and (d) $p = 1.4$ GPa.

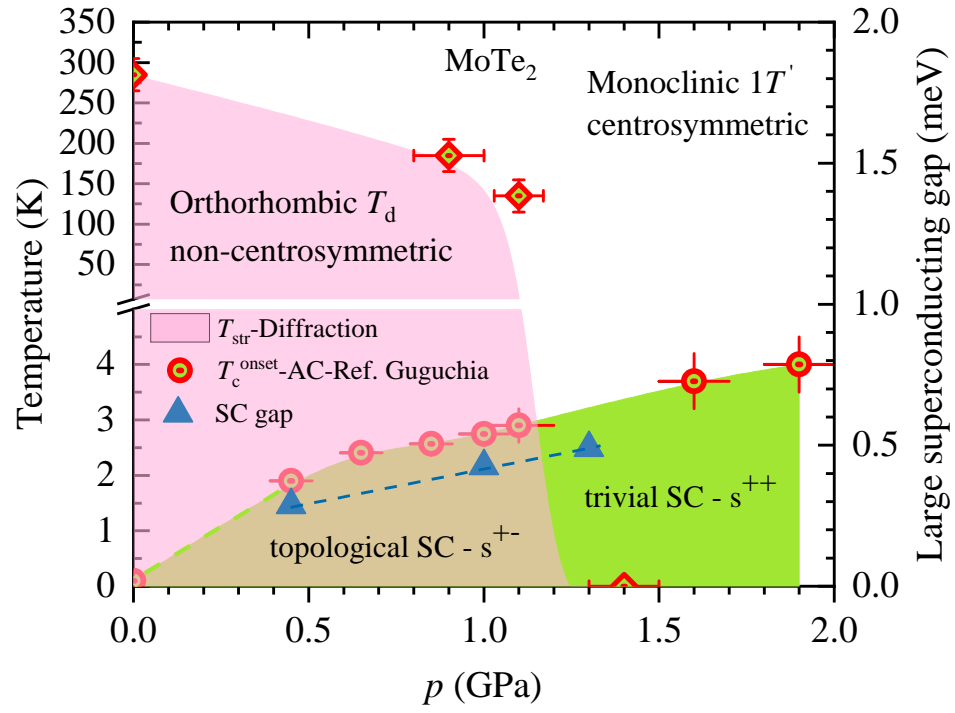


Figure 4: (Color online) (a) The pressure dependence of the superconducting critical temperature T_c (the red circles), the large SC gap Δ_2 (the blue triangles) and the monoclinic to orthorhombic structural phase transition temperature T_{str} (the red diamonds). The T_c and the Δ_2 values are taken from Ref. 25.